

On the Cosmological Stability of the Higgs Instability

Valerio De Luca^a, Alex Kehagias^b, Antonio Riotto^a

^a *Département de Physique Théorique and Centre for Astroparticle Physics (CAP),
Université de Genève, Geneva, Switzerland*

^b *Physics Division, National Technical University of Athens, Athens, 15780, Greece*

Abstract

The Standard Model Higgs potential becomes unstable at large Higgs field values where its quartic coupling becomes negative. While the tunneling lifetime of our current electroweak vacuum is comfortably longer than the age of the universe, quantum fluctuations during inflation might push the Higgs over the barrier, forming patches which might be lethal for our universe. We study the cosmological evolution of such regions and find that, at least in the thin wall approximation, they may be harmless as they collapse due to the backreaction of the Higgs itself. The presence of the Standard Model Higgs instability can provide a novel mechanism to end inflation and to reheat the universe through the evaporation of the black holes left over by the collapse of the Higgs bubbles. The bound on the Hubble rate during inflation may be therefore relaxed.

arXiv:2205.10240v1 [hep-ph] 20 May 2022

Contents

1	Introduction	3
2	The dynamics in the interior of the Higgs bubbles	4
3	Setting the stage for the Higgs bubble evolution	8
4	The fate of the Higgs bubbles	12
5	Analytical insights	15
5.1	Beyond the thin wall limit	16
6	Implications and conclusions	17
A	The big crunch singularity and the Higgs dynamics	19
B	Initial radius outside the de Sitter Hubble radius	21
C	Comparison with the past literature	22

1 Introduction

It is well-known that the current measured values of the Higgs boson and top quark masses lead to the surprising and intriguing realization that, in the context of the Standard Model (SM) with no additional physics, our universe situates itself at the edge between stability and instability of the electroweak vacuum (for some recent studies, see Refs. [1–3]).

The SM Higgs potential develops an instability well below the Planck scale, at an energy scale around $\Lambda \sim 10^{12}$ GeV¹ (for a gauge-invariant definition of the instability scale, see Ref. [6]), but with a lifetime which is comfortably and exceedingly longer than the age of the universe.

The stability of the electroweak vacuum is however not at all guaranteed in the early universe, when the presence of an unbounded from below direction with negative energy may represent a threat. For instance, during inflation [7] the fluctuations δh of the Higgs field, if the latter has no direct coupling to the inflaton and is minimally coupled to gravity (and therefore effectively massless during inflation), may push the Higgs field away from our current electroweak vacuum and above the barrier [8] (see also Refs. [9–11] and, for a recent review, Ref. [12]). This happens if roughly

$$\delta h \sim \frac{H_0}{2\pi} \gtrsim \Lambda, \quad (1)$$

where H_0 is the inflationary Hubble rate, so that the survival probability for the Higgs to remain in our electroweak vacuum is exponentially suppressed with time, $P_{\text{surv}} \sim \exp(-H_0^3 t/32\Lambda^2)$ [8].² During (and after) inflation our universe would then be filled up by spherical bubbles containing large values of the Higgs field probing the unstable region. It was concluded in Ref. [11] that such anti-de Sitter patches would be lethal for our universe: at the end of inflation such regions with negative vacuum energy density would expand at the speed of light and eventually engulf all space of our universe. This leads to the requirement that the probability to find an expanding anti-de Sitter bubble in our past light-cone must be negligible, thus deriving a strong upper bound on the Hubble constant during inflation (see also Refs. [17, 18])

$$H_0 \lesssim 5 \cdot 10^{-2} \Lambda. \quad (2)$$

The goal of this paper is to revisit the issue of the Higgs instability during inflation. We will show that the Higgs bubbles, originated by the fact that the Higgs fluctuations push the Higgs over the barrier, in fact may collapse due to the backreaction of the dynamics of the Higgs itself in the thin wall limit, an effect which has not been previously accounted for in the literature. Our findings indicate that the presence of the SM Higgs instability may not represent a danger for our universe. On the contrary, we will show that it offers a novel way to end inflation, to reheat our universe and to start the standard radiation-dominated phase.

¹Such a value is estimated taking into account the new measurement of the top quark mass, obtained by combining the latest Particle Data Group average [4] with the new CMS result [5].

²The probability of the Higgs vacuum decay may be enhanced in the presence of primordial black holes with masses $\lesssim 10^5 M_{\text{Pl}}$ (where $M_{\text{Pl}}^2 = 1/8\pi G$ is the reduced Planck mass) [13–16].

The paper is organised as follows. In Section 2 we discuss the dynamics in the interior of the Higgs bubbles. In Sections 3, 4 and 5 we analyse the fate of the Higgs bubbles and we conclude in Section 6. Three Appendices are devoted to technical details.

2 The dynamics in the interior of the Higgs bubbles

In this Section we are going to discuss the dynamics in the interior of the bubbles which are formed when the Higgs field, due to the stochastic fluctuations during inflation, overcomes the barrier of its potential and rolls down the potential along the unbounded from below direction.

The background interior metric describes in full generality (to include the case of a Higgs jumping deep enough that the total initial energy density is negative) a $O(1, 3)$ symmetric open Friedmann-Robertson-Walker (FRW) universe and is given by

$$ds_-^2 = -d\eta^2 + a^2(\eta) \left(d\chi^2 + S^2(\chi) d\Omega_2^2 \right), \quad S(\chi) = \sinh \chi, \quad (3)$$

where $d\Omega_2^2$ is the metric on the unit two-sphere and $a(\eta)$ denotes the scale factor in terms of the time coordinate η in the interior of the bubble. The equation of motion of the Higgs field is given by

$$h'' + 3\frac{a'}{a}h' - \frac{\nabla^2 h}{a^2} + \frac{\partial V_{\text{eff}}}{\partial h} = 0, \quad (4)$$

where the prime indicates differentiation with respect to η and V_{eff} is the effective Higgs potential. The equation of motion for the scale factor reads

$$\begin{aligned} (a')^2 &= 1 + \frac{a^2 \rho}{3M_{\text{Pl}}^2}, \\ \rho &= \frac{1}{2}(h')^2 + \frac{1}{2} \frac{(\nabla h)^2}{a^2} + V_{\text{eff}}. \end{aligned} \quad (5)$$

Since the Higgs values we will be considering probe the instability region, we will assume the quartic coupling to be negative at large Higgs field values. For our purposes one can assume the simplified expression for the Higgs potential

$$V_{\text{eff}} = V_0 - \frac{\lambda(h)}{4} h^4, \quad (6)$$

in terms of an inflation vacuum energy V_0 and the running quartic coupling [11]

$$\lambda(h) \simeq \frac{0.16}{(4\pi)^2} \ln \left(\frac{h^2}{\Lambda^2 \sqrt{e}} \right). \quad (7)$$

To properly solve the system of coupled differential equations, including the spatial dependence of the Higgs field, we have performed a lattice calculation making use of the program LATTICEASY, where the fields and its derivatives are evaluated on a spatial grid with evenly spaced points, in an expanding background [19]. The use of a lattice simulation which fully

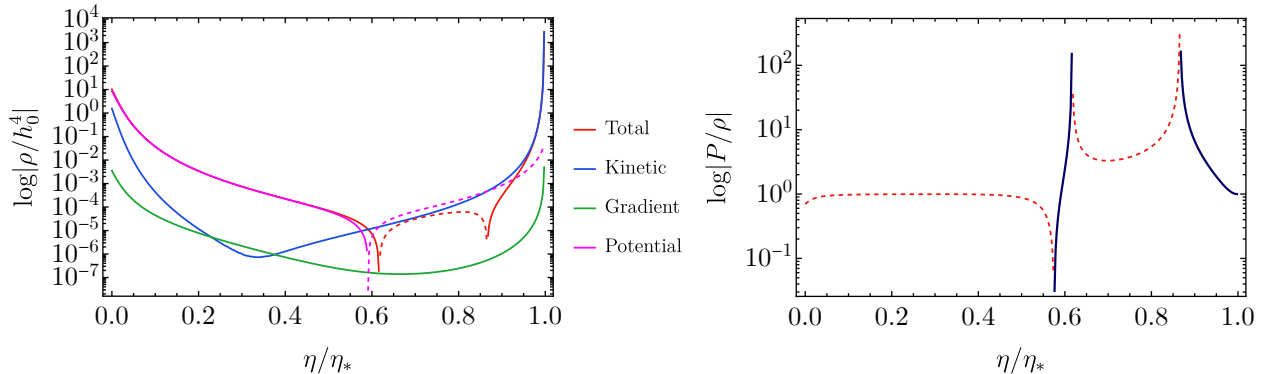


Figure 1: Left: Behaviour of the different components of the energy density with time. We have chosen $H_0/M_{\text{Pl}} = 10^{-4}$, $h_0 = H_0$, $h'(0) = 0$ and $a_0 = 1$. Dashed lines indicate a negative energy density. Right: The corresponding equation of state as a function of time, where P indicates the pressure density.

accounts for non-linear effects is necessary to properly include the effects of the spatial perturbations of the Higgs field. Indeed, due to the presence of the negative quartic term in the potential, the Higgs perturbations may experience in principle the phenomenon of tachyonic instability [20].

Let us call h_0 the initial value of the Higgs field at $\eta = 0$ when the bubble forms. Typically we expect $h_0 \sim H_0/2\pi$, where $H_0^2 = V_0/3M_{\text{Pl}}^2$, and zero velocity $h'(0) = 0$ over a Hubble distance H_0^{-1} , but our general results are independent from these assumptions. The Higgs bubble will therefore form with positive energy density inside dominated by the vacuum energy. Negative energy densities would require $h_0^2 \gtrsim (H_0 M_{\text{Pl}}/\lambda^{1/2})$, which is highly improbable (for our analytical approaches, in the following we will simplify the Higgs potential by a simpler form $-\lambda h^4/4$, with $\lambda > 0$).

In Fig. 1 we plot the total energy density of the system and its various components (left) and the corresponding equation of state (right). We highlight three points. First of all, the dynamics is characterized by the presence of a singularity point at $\eta = \eta_*$, whose origin we will discuss later on. Secondly, the contribution from the Higgs gradient energy density (computed through LATTICEEASY by averaging over distances larger than $1/(\sqrt{\lambda}h_0)$) is always subdominant compared to the Higgs kinetic and potential energy densities. Thirdly, while at the beginning the energy density is dominated by the inflation vacuum energy, the energy density becomes first negative, when the Higgs potential energy dominates due to the negative quartic coupling, and subsequently positive when the energy density of the system is dominated by the kinetic energy density of the Higgs field. Notice also that, at this stage, the potential energy density grows much more slowly than the kinetic energy density.

Since the fully non-linear solution of the dynamics shows that the gradient energy density of the Higgs is negligible, we are allowed to describe the dynamics of the scale factor and the Higgs field in the interior of the bubble and to explain the origin of the singularity point without including such a contribution.

We are dealing therefore with a typical potential with an unbounded from below direction.

The equations of motion reduce to

$$\begin{aligned} h'' + 3\frac{a'}{a}h' + \frac{\partial V_{\text{eff}}}{\partial h} &= 0, \\ (a')^2 &= 1 + \frac{a^2}{3M_{\text{Pl}}^2} \left(\frac{1}{2}(h')^2 + V_{\text{eff}} \right), \end{aligned} \quad (8)$$

while the equation for the conservation of the energy density reads

$$\frac{d\rho}{d\eta} = \frac{d}{d\eta} \left(\frac{1}{2}(h')^2 + V_{\text{eff}} \right) = -3\frac{a'}{a}(h')^2. \quad (9)$$

The total energy density is increasing for contracting ($a' < 0$) or decreasing for expanding ($a' > 0$) universe.

After the formation of the Higgs bubble, its interior still experiences a stage of inflation, with the scale factor growing exponentially. The Higgs motion is classical if in a Hubble time the motion is dominated by the classical friction rather than by the quantum one. If so, the Higgs scalar field slowly rolls down from the top of the effective potential satisfying the equation

$$3H_0 h' \simeq \lambda h^3. \quad (10)$$

The classical motion beats the quantum one if [21]

$$\delta h_c \sim \frac{h'}{H_0} \sim \frac{\lambda h_0^3}{3H_0^2} \gtrsim \delta h_q \sim \frac{H_0}{2\pi}, \quad (11)$$

or

$$h_0^3 \gtrsim \frac{3H_0^3}{2\pi\lambda}, \quad (12)$$

which we will assume from now on. The solution of Eq. (10) is given by

$$h^2(\eta) \simeq \frac{h_0^2}{1 - 2\lambda h_0^2 \eta / 3H_0}. \quad (13)$$

The quartic term starts dominating over the vacuum energy (and the total energy becomes negative, before getting positive again), $\lambda h^4 \sim M_{\text{Pl}}^2 H_0^2$, around the singularity time

$$\eta_* \simeq \frac{3H_0}{2\lambda h_0^2}. \quad (14)$$

The Higgs zero mode value at this stage is such that $h^2 \sim (M_{\text{Pl}} H_0 / \lambda^{1/2}) \ll M_{\text{Pl}}^2$. Subsequently, the speed of the Higgs field rapidly increases and in a Hubble time reaches the singularity. To understand this point, let us neglect for a moment the effects of the expansion of the universe in the Higgs equation of motion such that, at large values of the Higgs field, we may write [22]

$$(h')^2 \simeq 2(V_0 - V_{\text{eff}}), \quad (15)$$

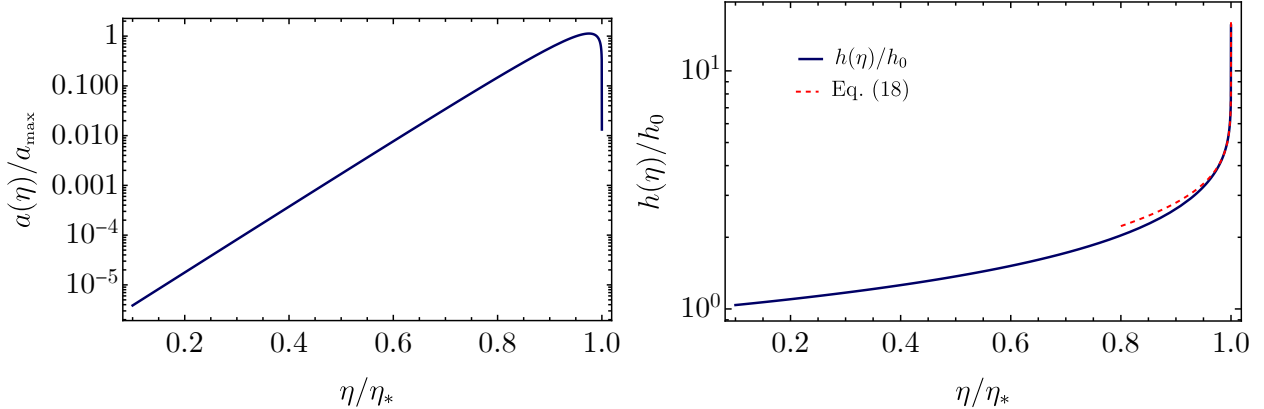


Figure 2: Left: time behaviour of the scale factor close to the singularity, normalised with respect to its maximum value a_{\max} . Right: time behaviour of the Higgs zero mode close to the singularity. We have chosen $H_0/M_{\text{Pl}} = 10^{-4}$, $h_0 = H_0$, $h'(0) = 0$ and $a_0 = 1$.

and the acceleration of the universe is dictated by the equation

$$\frac{a''}{a} = \frac{1}{3M_{\text{Pl}}^2} [V_{\text{eff}} - (h')^2] \simeq \frac{1}{3M_{\text{Pl}}^2} (3V_{\text{eff}} - 2V_0) \simeq -\frac{\lambda}{4M_{\text{Pl}}^2} h^4. \quad (16)$$

At large Higgs values the universe starts moving with ever growing negative acceleration. If one reintroduces back the expansion of the universe, the Higgs speed becomes even smaller, and the deceleration is even greater. As a result, the expansion slows down and the universe starts contracting. At this stage the friction term $3(a'/a)h'$ in the equation of motion of the Higgs becomes negative, which causes the Higgs to grow and leads to a rapid collapse of the universe [22]. Therefore, once the universe approaches the turning point where the total energy density vanishes ($a' = 0$), it begins collapsing, and the total energy density becomes positive again. During the last phase, the energy density is therefore dominated by the Higgs kinetic term and we may write

$$\begin{aligned} (a')^2 &\simeq \frac{a^2}{3M_{\text{Pl}}^2} \frac{1}{2} (h')^2, \\ \frac{h''}{h'} &= -3 \frac{a'}{a}, \end{aligned} \quad (17)$$

whose solutions are

$$a(\eta) \simeq a_0 (\eta_* - \eta)^{1/3}, \quad (18)$$

$$h(\eta) \simeq h_0 + M_{\text{Pl}} \sqrt{\frac{2}{3}} \ln \left(\frac{\eta_* - \eta_0}{\eta_* - \eta} \right). \quad (19)$$

These behaviours are reproduced by the numerical results plotted in Fig. 2 where we show the evolution of the scale factor and the Higgs field. Notice also that the potential energy density grows only as $\ln^4(\eta_* - \eta)$, that is much smaller than the kinetic energy density which scales like $1/(\eta_* - \eta)^2$ around the pole. This explains the hierarchy between the two contributions in Fig. 1.

The curvature term is always negligible because of the previous inflationary stage. The universe is therefore effectively flat at this epoch. Furthermore, the Higgs field close to the singularity rolls down slowly, only logarithmically. We assume that, in the case in which there is a new deeper minimum at some high value of the Higgs field, say at scales larger than the Planck mass (possibly generated by a higher-dimensional operator of the form h^6/M_{Pl}^2), the scale factor contracts before it is reached.

We are now in the position to go back to the issue of the Higgs gradient energy and explain analytically why it is smaller than the other components. During the period in which the scale factor expands exponentially, the gradients of the Higgs field are suppressed and so it is their contribution to the Higgs total energy density compared to the other components when the Higgs starts rolling down its potential. The equation of motion of the rescaled Higgs field $\tilde{h}_k = ah_k$ in Fourier space and in terms of the comoving time $d\tilde{\eta} = d\eta/a$ reads at the linear level

$$\frac{d^2\tilde{h}_k}{d\tilde{\eta}^2} + \left(k^2 - \frac{1}{a} \frac{d^2a}{d\tilde{\eta}^2} - 3\lambda h^2(\tilde{\eta})a^2 \right) \tilde{h}_k = 0. \quad (20)$$

By appropriately choosing the initial condition we can set $\tilde{\eta} \sim (\eta_* - \eta)^{2/3}$ close to the singularity. As the scale factor contracts, the tachyonic mass squared gets smaller and smaller, and modes which are outside the comoving Hubble radius $\tilde{\mathcal{H}}^{-1} = a/(da/d\tilde{\eta}) \sim \tilde{\eta}$ have an amplitude $\tilde{h}_k \sim a$. During the contraction phase more modes exit the Hubble radius, as the physical wavelength $a/k \sim (\eta_* - \eta)^{1/3}$ scales slower than the physical Hubble radius $a/a' \sim (\eta_* - \eta)$, and one expects the contribution to the gradient energy density to be smaller than the kinetic energy density. To estimate the former we consider the Higgs fluctuations which have an amplitude given roughly by $h_k \sim H_0/k^{3/2}$ [21], as they inherit the de Sitter power spectrum during the slow-roll phase of the Higgs field. Correspondingly, the Higgs gradient energy density scales such that

$$\frac{(\nabla h)^2}{2a^2} \sim \int^{1/\tilde{\eta}} \frac{d^3k}{(2\pi)^3} \frac{k^2 |h_k|^2}{2a^2} \sim \frac{H_0^2}{\tilde{\eta}^2 a^2} \sim \frac{H_0^2}{(\eta_* - \eta)^2} \ll \frac{1}{2} (h')^2 \sim \frac{M_{\text{Pl}}^2}{(\eta_* - \eta)^2}. \quad (21)$$

Our numerical results, including the same time dependence of the Higgs gradient and kinetic energy densities, confirm our analytical findings.

3 Setting the stage for the Higgs bubble evolution

The goal of this Section is to set the stage for the description of the dynamics of the Higgs bubbles once they are formed, in order to understand if the Higgs bubbles may or not pose a threat for our current universe.

The Higgs bubble materializes as a spherically symmetric object. At its interior the metric is given in Eq. (3), while the external space will be that of Schwarzschild-de Sitter with metric

$$ds_+^2 = -f(r)dt^2 + \frac{dr^2}{f(r)} + r^2 d\Omega_2^2, \quad f(r) = 1 - \frac{2GM}{r} - H_0^2 r^2. \quad (22)$$

The bubble wall is located at

$$\chi = X(\tau), \quad (23)$$

as seen from the inside geometry and at

$$r = R(\tau) \quad (24)$$

from the outside geometry. The intrinsic bubble metric is

$$d\sigma^2 = \gamma_{ij}d\xi^i d\xi^j = -d\tau^2 + R^2(\tau)d\Omega_2^2, \quad (25)$$

where $\xi^i = (\tau, \theta, \phi)$ are the bubble worldvolume coordinates. The induced metrics on the bubble from the two sides are

$$d\sigma_-^2 = -\left(\dot{T}_-^2 - a^2\dot{X}^2\right) d\tau^2 + a^2 S^2(X)d\Omega_2^2, \quad (26)$$

from the interior and

$$d\sigma_+^2 = -\left(f(R)\dot{T}_+^2 - \frac{\dot{R}^2}{f(R)}\right) d\tau^2 + R^2 d\Omega_2^2, \quad (27)$$

from the exterior and we have used a dot to indicate derivatives with respect to τ . We call the attention of the reader on the fact that times are dubbed as follows

$$\begin{aligned} \text{interior : } \eta &= \eta(\tau) = T_-(\tau), \\ \text{exterior : } t &= t(\tau) = T_+(\tau). \end{aligned} \quad (28)$$

The two metrics (26) and (27) should coincide with the intrinsic bubble metric of Eq. (25), leading to the conditions

$$\dot{T}_-^2 - a^2\dot{X}^2 = 1, \quad (29)$$

$$f(R)\dot{T}_+^2 - \frac{\dot{R}^2}{f(R)} = 1, \quad (30)$$

$$\frac{R}{aS} = 1. \quad (31)$$

We apply the Israel matching conditions [23] for the extrinsic curvature of the bubble

$$K_{ij}^+ - K_{ij}^- = -\frac{1}{M_{\text{Pl}}^2} \left(S_{ij} - \frac{1}{2} S_k^k \gamma_{ij} \right), \quad (32)$$

where

$$K_{ij} = e_i^\mu e_j^\nu \nabla_\mu n_\nu, \quad (33)$$

n^μ being the normal to the bubble hypersurface, and

$$S_{ij} = -2\sigma\gamma_{ij} \quad (34)$$

is the surface stress-energy tensor of the bubble wall in terms of its tension σ . The projection tensor e_i^μ is defined as

$$e_i^\mu = \frac{\partial x^\mu}{\partial \xi^i}. \quad (35)$$

To solve for the dynamics of the Higgs bubble wall analytically, we take the thin wall approximation³, which assumes that any variation of the Higgs scalar field along the wall occurs only on length scales much larger than the wall thickness, that is $\partial_\mu h \sim n_\mu$. It follows that the bubble tension is constant with time [24], a starting point we will take from now on. Admittedly, this is a strong assumption and a fully non-linear numerical analysis would be required to go beyond the thin wall approximation.

If u^μ is the velocity vector along a geodesic, then the normal n^μ is defined as

$$u^\mu = \frac{dx^\mu}{d\tau}, \quad u^\mu u_\mu = -1, \quad n^\mu u_\mu = 0, \quad n^\mu n_\mu = 1. \quad (36)$$

These conditions specify the normal vector, in an obvious notation, as

$$n_-^\mu = \left(a\dot{X}, \frac{\dot{T}_-}{a}, 0, 0 \right), \quad n_+^\mu = \left(\frac{\dot{R}}{f}, f\dot{T}_+, 0, 0 \right). \quad (37)$$

Using the above normal vectors, the extrinsic curvature turns out to be

$$K_{\theta\theta}^- = \dot{T}_- a S \frac{\partial S}{\partial \chi} + \dot{X} a^2 a' S^2, \quad K_{\phi\phi}^- = \sin^2 \theta K_{\theta\theta}^-, \quad (38)$$

and similarly,

$$K_{\theta\theta}^+ = f R \dot{T}_+, \quad K_{\phi\phi}^+ = \sin^2 \theta K_{\theta\theta}^+. \quad (39)$$

The Israel matching condition (32) leads then to the equation

$$f R \dot{T}_+ - \dot{T}_- a S \frac{\partial S}{\partial \chi} - \dot{X} a' a^2 S^2 = -\frac{\sigma R^2}{2M_{\text{Pl}}^2}, \quad (40)$$

which can be written as

$$f \dot{T}_+ - \dot{T}_- \frac{\partial S}{\partial \chi} - \dot{X} a' a S = -\frac{\sigma R}{2M_{\text{Pl}}^2}. \quad (41)$$

From Eq. (31) we find that

$$\dot{X} = \frac{1}{a^2 \frac{\partial S}{\partial \chi}} \left(-a' \dot{T}_- R + a \dot{R} \right), \quad (42)$$

³This is the same assumption taken in Ref. [11] again to make the problem tractable analytically.

so that Eq. (29) is expressed as

$$\dot{T}_-^2 - \frac{1}{\left(\frac{\partial S}{\partial \chi}\right)^2} \left(-\frac{a'}{a} \dot{T}_- R + \dot{R}\right)^2 = 1. \quad (43)$$

Solving Eq. (43) for \dot{T}_- and using it together with Eq. (42) in the Israel matching condition Eq. (41), we get

$$\left(\dot{R}^2 + 1 + \frac{R^2}{a^2} - \frac{a'^2}{a^2} R^2\right)^{1/2} = \epsilon \left(f + \dot{R}^2\right)^{1/2} + \frac{\sigma R}{2M_{\text{Pl}}^2}, \quad (44)$$

where $\epsilon = \text{sign } \dot{T}_+$. With the help of the Friedmann equation (8), we can write Eq. (44) as⁴

$$\dot{R}^2 + V(R) = -1, \quad (45)$$

where

$$V(R, \eta) = -\frac{k_1}{R^4} - \frac{k_2}{R} - k_3 R^2 \quad (46)$$

is a time-dependent potential with

$$k_1 = \frac{1}{16\pi^2} \frac{M^2}{\sigma^2}, \quad k_2 = \frac{M(\rho_c - \rho)}{6\pi \sigma^2}, \quad k_3 = \frac{\rho}{3M_{\text{Pl}}^2} + \frac{(\rho - \rho_c)^2}{9\sigma^2}. \quad (47)$$

We have defined the constant ρ_c as

$$\rho_c = \frac{3\sigma^2}{4M_{\text{Pl}}^2} + 3M_{\text{Pl}}^2 H_0^2. \quad (48)$$

From Eq. (45) one can write the expression for the mass M as

$$M = \frac{4}{3}\pi R^3(\rho - \rho_c) + 4\pi\sigma R^2 \left(1 - \frac{\rho}{3M_{\text{Pl}}^2} R^2 + \dot{R}^2\right)^{1/2}, \quad (49)$$

which is a constant of motion whose sign is not a priori defined. However, negative masses, once the bubble collapses, would leave behind a naked singularity, which is in contradiction with the Cosmic Censorship theorem [25], for more details see Appendix A. Notice also that, as we will discuss later on, neither the magnitude nor the sign of the mass are relevant for the dynamics close to the singularity.

Summarizing, in order to determine the dynamics of the bubble, one should solve the following equations

$$f(R)\dot{T}_+^2 - \frac{\dot{R}^2}{f(R)} = 1, \quad (50)$$

$$\dot{T}_-^2 - \frac{1}{\left(\frac{\partial S}{\partial \chi}\right)^2} \left(-\frac{a'}{a} \dot{T}_- R + \dot{R}\right)^2 = 1, \quad (51)$$

$$\dot{R}^2 + V(R) = -1. \quad (52)$$

⁴Notice that Eq. (45) does not depend on the value of the spatial curvature of the internal spacetime, i.e. it is valid also for $S(\chi) = \chi$ or $S(\chi) = \sin \chi$.

4 The fate of the Higgs bubbles

After setting the stage to study their dynamics, we are now in the position to investigate the fate of the Higgs bubbles. We do it first numerically and then offer a more analytical insight in the next Section. It is convenient to regard R and T_+ as functions of $\eta = T_-$. In this case, Eqs. (50-52) are written as

$$R'^2 = -(1+V) \left(1 - \frac{1}{1 + \frac{R^2}{a^2}} \left(-\frac{a'}{a} R + R' \right)^2 \right), \quad (53)$$

$$T_+'^2 = \frac{1}{f} \left(1 + \frac{R'^2}{f} \left(1 - \frac{1}{1 + \frac{R^2}{a^2}} \left(-\frac{a'}{a} R + R' \right)^2 \right)^{-1} \right), \quad (54)$$

and

$$\dot{T}_-^2 = \left(1 - \frac{1}{1 + \frac{R^2}{a^2}} \left(-\frac{a'}{a} R + R' \right)^2 \right)^{-1}. \quad (55)$$

Notice that these set of equations exactly reproduce Eqs. (B.14-B.16) in Appendix B for the case of initial bubble radii larger than the Hubble radius by simply setting $f = 1$. Solving for R' through Eq. (53), we find the most relevant equation of the paper

$$R' = -\frac{aa'(1+V)R}{R^2 - a^2V} \pm \frac{1}{R^2 - a^2V} \sqrt{(1+V)(a^2 + R^2)(a^2V - R^2(1 - a'^2))}. \quad (56)$$

Now the strategy is simple. Eq. (56) is a differential equation which provides $R(\eta)$. Then the solution can be used in Eq. (54) to determine T_+ . Finally, Eq. (55) determines $\eta(\tau)$ which can be used to specify the solutions as $R(\eta(\tau))$ and $t(\eta(\tau))$.

The behaviour of the bubble radius is shown in Fig. 3 for different initial conditions. Our results indicate that the Higgs bubbles expand exponentially at the beginning, but end up contracting and they do so by following the same time dependence of the internal scale factor. In particular, the bubbles start increasing their sizes, have a turning point when $R' = 0$, and at the final stage they collapse to zero size, leaving a singularity behind. Eq. (53) shows that the bubble wall has a turning point not only when $(1+V)$ vanishes, but also when the second parenthesis does so. Indeed, as we will see later on, at the turning point V is very large in absolute value and R' approaches zero because of the growing behaviour of \dot{T}_- . Our results are not sensitive to the bubble mass M and to the choice of the initial bubble radius in units of H_0^{-1} .

To understand better the behaviour of the bubble wall, let us rewrite Eq. (56) in the following form

$$R'^2 + \mathcal{V}(R) = -1, \quad (57)$$

by defining the bubble potential

$$\mathcal{V}(R) \equiv - \left[-\frac{aa'(1+V)R}{R^2 - a^2V} \pm \frac{1}{R^2 - a^2V} \sqrt{(1+V)(a^2 + R^2)(a^2V - R^2(1 - a'^2))} \right]^2 - 1. \quad (58)$$

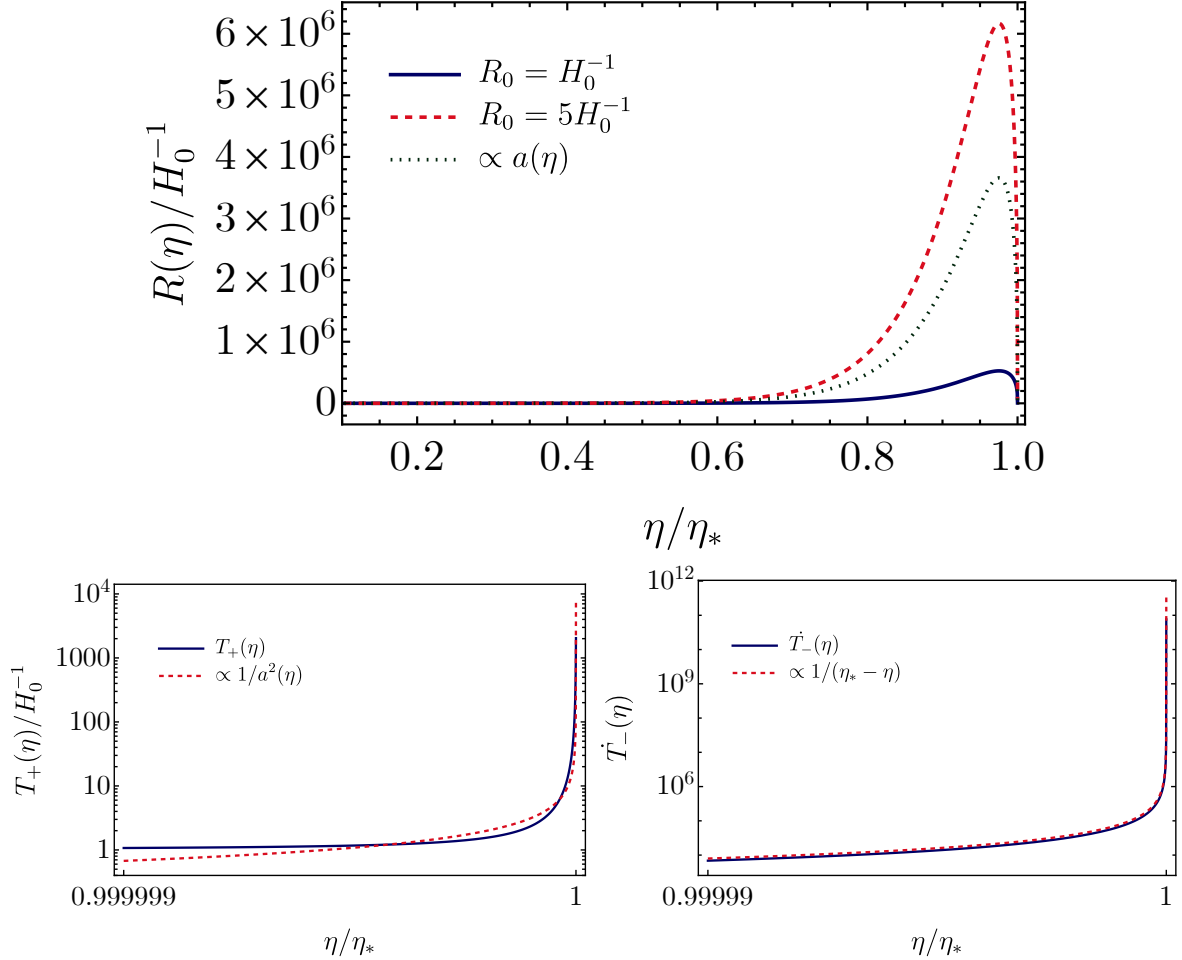


Figure 3: The evolution of the bubble wall radius (top), and external and internal times (bottom). We have chosen $H_0/M_{\text{Pl}} = 10^{-4}$, $h_0 = H_0$, $h'(0) = 0$ and we have renormalised the initial value of the scale factor to unity at the beginning of the Higgs dynamics.

For a fixed radial coordinate R , the bubble potential depends on time both through the scale factor a and the potential V . To show its time dependence we have to consider therefore the time evolution inside the bubble. At initial times, the radius of the bubble can be taken of the order of the inverse Hubble horizon, that is $R_0 \sim H_0^{-1}$, and the Higgs fluctuations are of the order of $h_0 \sim H_0/2\pi$. Our results do not depend however from this choice. The wall tension and mass are then given by [11]

$$\sigma \sim \frac{\sqrt{\lambda}}{(2\pi)^3} H_0^3 \quad \text{and} \quad M \sim \frac{\sqrt{\lambda}}{(2\pi)^2} H_0, \quad (59)$$

and, as already pointed out above, they do not depend on time. At the initial stage the typical

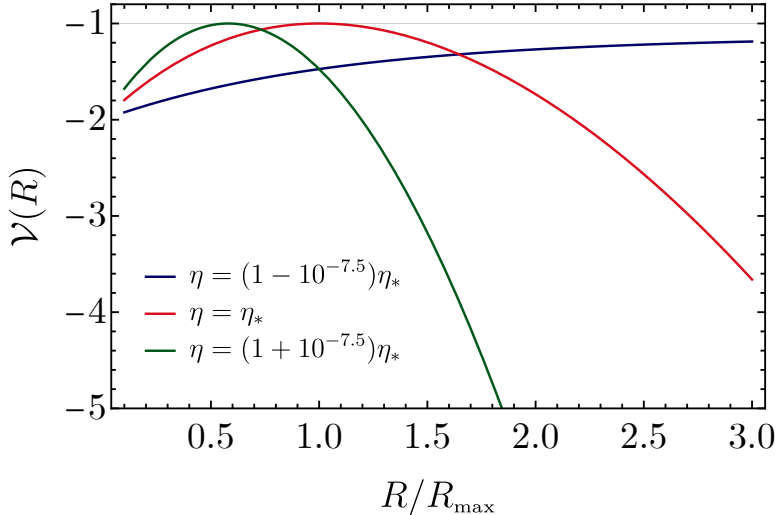


Figure 4: Illustrative plot of the bubble potential $\mathcal{V}(R)$ in terms of the bubble radius R at different times η close to the turning point.

parameters which enter in the potential V are then

$$\begin{aligned}
 k_1 &= \frac{1}{16\pi^2} \frac{M^2}{\sigma^2} \sim \frac{1}{4H_0^4}, \\
 k_2 &= \frac{M(\rho_c - \rho)}{6\pi \sigma^2} \sim \frac{\sqrt{\lambda}}{6\pi H_0}, \\
 k_3 &= \frac{\rho}{3M_{\text{Pl}}^2} + \frac{(\rho - \rho_c)^2}{9\sigma^2} \sim H_0^2 - \frac{\lambda}{(2\pi)^4} \frac{H_0^4}{M_{\text{Pl}}^2} + \frac{\lambda H_0^2}{9(2\pi)^2} \sim H_0^2,
 \end{aligned} \tag{60}$$

and one can appreciate the hierarchy

$$\frac{2GM}{R_0} \sim \frac{\sqrt{\lambda}}{(2\pi)^3} \frac{H_0^2}{M_{\text{Pl}}^2} \ll H_0^2 R_0^2. \tag{61}$$

Once the equations of motion for the scale factor and scalar field have been solved, one can plug the solutions in the effective potential and show its behaviour in terms of the bubble radius, for different times. The result is shown in Fig. 4. The crucial information one gets is that, close to the big crunch η_* , the effective potential crosses -1 . At that stage the bubble velocity R' becomes zero, and thus the bubble radius starts contracting from its maximum value R_{max} following the behaviour already shown in Fig. 3. Furthermore, after reaching the turning point, the potential gets squeezed to smaller radii. Our results can be understood from the Newtonian point of view. In the limit of $(\sigma/M_{\text{Pl}})^2 \ll \rho$ and $\dot{R} \simeq 0$, the bubble mass (49) receives two contributions, one from the volume term and the other from the surface term. Being both positive, the bubble contracts.

We stress that our findings do not change by assuming different initial conditions. In particular, close to the pole the value of the bubble mass M is not relevant for the behaviour of the bubble radius, thus changing only slightly the value of the radius at the turning point R_{max} . We devote the next Section to describe these behaviours analytically.

5 Analytical insights

To understand the previous results analytically, let us analyse the dynamics using Eq. (56). During the phase when the vacuum energy dominates and the internal scale factor grows exponentially, $a(\eta) \sim \exp(H_0\eta)$, the bubble wall expands exponentially as well, since Eq. (56) reduces to $R'/R \simeq a'/a$. Let us now see what happens when the big crunch for the scale factor at $\eta = \eta_*$ is approached for typical initial conditions. As we have previously proven, close to the collapse, the kinetic energy of the Higgs field is dominating and we have

$$a \sim (\eta_* - \eta)^{1/3}. \quad (62)$$

From Eq. (8) we find that the energy density scales like

$$\rho \sim \frac{1}{a^6} \sim \frac{1}{(\eta_* - \eta)^2}. \quad (63)$$

Eq. (56) simplifies considerably as one takes the limit of large V . Indeed, inspecting Eq. (47) we see that close to the singularity

$$\frac{k_1}{R^4} \sim \frac{M^2}{\sigma^2} \frac{1}{R^4} \sim \frac{1}{a^4} \ll \frac{k_2}{R} \sim \frac{M\rho}{\sigma^2} \frac{1}{R} \sim \frac{1}{a^7} \ll k_3 R^2 \sim \frac{\rho^2}{\sigma^2} R^2 \sim \frac{1}{a^{10}}, \quad (64)$$

so that

$$V \sim -\rho^2 R^2 \sim -\frac{R^2}{(\eta_* - \eta)^4} \quad (65)$$

and the mass M of the bubble does not play any crucial role in the dynamics. Eq. (56) reduces to

$$R' \approx \frac{a'}{a} R \pm \frac{\sqrt{a^2 + R^2}}{-a}, \quad (66)$$

which, inserted in Eq. (53), shows that the bubble wall velocity becomes zero as the second parenthesis vanishes. Eq. (66) can be solved at leading order close to the singularity as

$$R(\eta) \sim a(\eta) \sim (\eta_* - \eta)^{1/3}. \quad (67)$$

The full numerical result also confirms the analytical expectation that, close to the singularity, the bubble size and the scale factor have the same time dependence, see Fig. 3. Plugging this solution into the equations for T_+ and T_- one easily finds that, close to the singularity,

$$T_+'^2 \sim -V \sim \frac{R^2}{(\eta_* - \eta)^4}, \quad (68)$$

leading to the external observer time

$$t = T_+(\eta) \sim \frac{1}{a^2} \sim \frac{1}{(\eta_* - \eta)^{2/3}}. \quad (69)$$

The external observer sees the bubble collapsing with a time behaviour

$$R(t) \sim t^{-1/2} \quad \text{for } t \rightarrow \infty. \quad (70)$$

Similarly, we find

$$\dot{T}_-^2 \sim -\frac{V}{R^2} \sim \frac{1}{(\eta_* - \eta)^2} \quad \text{or } \tau \sim (\eta_* - \eta)^2 \sim t^{-3}, \quad (71)$$

in such a way that the bubble contracts for the proper observer on the bubble as $R(\tau) \sim \tau^{1/6}$ around the singularity $\tau = 0$.

The difference between our results and those found in Ref. [11] is that there the potential $V(R)$ was considered to be time-independent, since it was assumed that the Higgs field was already sitting at a deep minimum at some value $h \gtrsim M_{\text{Pl}}$, thus neglecting the time-dependent dynamics of the Higgs. In the interior of the bubble the geometry was exactly anti-de Sitter and in the exterior exactly de Sitter or Minkowski. In such a case, the backreaction of the dynamics of the Higgs, which makes the total energy density within the bubble positive and large close to the singularity, is absent and solutions with expanding bubble walls can be found, see Appendix C for a more detailed discussion. This can be understood also in the Newtonian limit where the gravitational self-energy of the wall can be neglected. Large bubbles grow indefinitely because the system gains energy in the process if the interior energy density is negative, as in Ref. [11]. In our case, bubbles shrink for opposite energetic reasons when the energy density becomes positive due to the Higgs dynamics. Notice also that, during the contraction phase, the vacuum energy of the inflaton field does not play any role. We therefore expect that Higgs bubbles which are formed at the very end of inflation will contract even if they are surrounded by an asymptotic Minkowski spacetime immediately after inflation.

5.1 Beyond the thin wall limit

Our considerations are valid in the thin wall limit and going beyond it would require a full numerical approach to include the spatial and time dependence of the Higgs configuration, taking into account the time dependence of the bubble wall thickness, the surface energy density, and the surface tension. However, it has been suggested that, in the case of a thick bubble, even though the details of the collapse may change (for instance the effective wall tension and the bubble contraction velocity), the results could be qualitatively similar to the thin wall ones [26–30].

This might be confirmed by the following arguments. If the Higgs bubble wall thickness is non-vanishing, one has to impose the Israel matching conditions for the extrinsic curvature of the bubble also on the $\tau\tau$ -component. However, using the covariant conservation of the energy-momentum tensor, this turns out to be the time derivative of the $\theta\theta$ -component [28, 29] and our system of equations can be used upon redefining an effective time dependent bubble wall tension. If the latter decreases in time, our analytical insights indicate that the collapse would persist, as the leading term in the potential V close to the singularity would scale like $V \sim k_3 R^2 \sim \rho^2 R^2 / \sigma^2$, even faster than $\sim \rho^2$. Consider now the more likely case that the

Higgs bubble wall tension increases. This may happen by (boldly) assuming a finite and time-independent thickness ΔR of the Higgs bubble wall [28,29], such that the tension would roughly scale with time as

$$\sigma \sim \rho \Delta R \sim \frac{\Delta R}{a^6}. \quad (72)$$

The various coefficients in the potential V would then have the behaviour close to the singularity

$$\begin{aligned} k_1 &= \frac{1}{16\pi^2} \frac{M^2}{\sigma^2} \sim 0, \\ k_2 &= \frac{M}{6\pi} \frac{(\rho_c - \rho)}{\sigma^2} \sim \frac{M}{M_{\text{Pl}}^2}, \\ k_3 &= \frac{\rho}{3M_{\text{Pl}}^2} + \frac{(\rho - \rho_c)^2}{9\sigma^2} \sim \frac{\rho}{M_{\text{Pl}}^2}, \end{aligned} \quad (73)$$

and one immediately deduces that the leading term in the potential V close to the singularity is $V \sim k_3 R^2 \sim \rho R^2 / M_{\text{Pl}}^2$, leading again to Eq. (66) and to a contracting behaviour of the bubble radius, $R \sim a$. We have checked numerically that the bubble radius indeed contracts also in this case. Notice that Eq. (72) is consistent with the perturbative expansion at first-order in the bubble thickness ΔR [28]

$$\sigma \sim \Delta R \left(\frac{\dot{R}^2}{R^2} + \frac{1}{R^2} \right) \sim \frac{\Delta R}{\tau^2} \sim \rho \Delta R \sim \frac{\Delta R}{a^6}, \quad (74)$$

where the third passage is valid since, in such a case, the time variables are related to each other by the scaling $\tau \sim (\eta_* - \eta)$. As stressed above, the resolution of the full problem requires the study of the spatial and time dependence of the Higgs configuration. If the bubble wall is not thin, we expect the Higgs configuration to be divided in three regions. In the internal contracting one the Higgs has large values and its positive kinetic energy density dominates. In the external region the Higgs vacuum expectation value is zero. In the middle region the Higgs interpolates between the two values. If the middle value goes down rapidly enough to continuously follow the internal value such that its energy density becomes positive, we expect the Higgs bubble wall to contract. In the thin wall limit the middle and interior regions coincide, and the Higgs bubble wall contracts following the collapse of the interior region.

6 Implications and conclusions

Assuming that the SM holds up to large energies, we have investigated the cosmological evolution of the Higgs field during inflation and reanalysed the issue of the stability of the electroweak vacuum. We have argued that the stability may be guaranteed thanks to the backreaction of the Higgs dynamics. The essential point is that, at the interior of the Higgs patches where the Higgs potential is unbounded from below, the Higgs kinetic energy quickly dominates and the bubble walls collapse following the internal scale factor towards the singularity.

This result, which is independent from the particular form of the Higgs potential at large values of the Higgs field in the unbounded from below region, is intimately connected with the fact that a period of cosmological inflation is incompatible with a universe dominated by a negative energy density. Indeed, after a period of inflation, the curvature term may be omitted and the Friedmann equation may not have a solution with negative energy density. In other words, the prediction of the inflationary cosmology is that we cannot end up in a space dominated by negative energy density [31]. When the interior of the bubble approaches the turning point, where the total energy density vanishes, it has to collapse in such a way that the total energy density becomes positive again. At the same time, the bubble wall follows the internal scale factor due to the dynamics of the Higgs field itself and collapses. Notice also that the null energy condition assures that, if the universe switches from expansion to contraction, it will not return to the regime of expansion later on, even including the backreaction of particle production.

The singularities left over by the collapse of the Higgs bubbles are hidden behind a black hole horizon according to the Cosmic Censorship theorem. This implies the following dynamics. Inflation starts and the Higgs fluctuations push the Higgs zero mode beyond the barrier after a fraction of one e-fold if $H_0 \gg \Lambda$. Subsequently inflation keeps going on for a number of e-folds of the order of $\eta_* H_0$, which is typically much larger than the minimum number of e-folds ~ 60 required to reproduce our observable flat universe. Afterwards, all Hubble regions of initial volume $\sim H_0^{-3}$ contained in the inflated region of volume $\sim H_0^{-3} \exp(3\eta_* H_0)$ collapse under the backreaction of the Higgs field which takes over the energy density, thus stopping inflation. Black holes form and populate the universe. Their typical mass is of the order of the Hubble rate during inflation and therefore rapidly evaporate with a time scale of the order of $\sim M^3/M_{\text{Pl}}^4 \sim H_0^3/M_{\text{Pl}}^4$. Thus, possibly and interestingly, the presence of the SM Higgs instability may offer a novel way to end inflation and to reheat the universe through minuscule primordial black holes if they evaporate completely (see also Ref. [32]). It will be interesting to investigate the consequences of such new dynamics.

Our findings indicate that the Hubble rate during inflation may be not bounded from above to be smaller than a fraction of the instability energy of the SM Higgs potential. This has implications for the possible future detection of primordial gravitational waves generated during inflation as their detection requires values of the Hubble rate much larger than the Higgs instability scale [33].

Finally, let us stress again that our results are based on some assumptions. First, as already remarked, the thin wall limit which allows a manageable analytical computation. It will be interesting and pressing to extend our results relaxing the thin wall hypothesis to understand if a thick wall can decouple the expansion of the Higgs bubble from the collapse of its inner region. Secondly, the hypothesis that the Higgs rolls down along the unbounded from below direction for a sufficiently large time to allow the Higgs kinetic energy to dominate and the Higgs bubble to collapse. We plan to investigate these issues in the next future.

Acknowledgments

We thank A. Strumia and N. Tetradis for interesting comments and discussions, G. Felder for insightful comments on the program LATTICEASY, and R. Bravo, J.R. Espinosa, G. Franciolini, G.F. Giudice, D. Racco, and L. Senatore for useful feedbacks. V.DL. and A.R. are supported by the Swiss National Science Foundation (SNSF), project *The Non-Gaussian Universe and Cosmological Symmetries*, project number: 200020-178787. A.K. is supported by the PEVE-2020 NTUA programme for basic research with project number 65228100.

A The big crunch singularity and the Higgs dynamics

We describe here the fate of a Higgs bubble and show that it ends up accommodating a singularity in its interior. We are inspired by Ref. [34], where the interested reader can find additional details. Let us consider a scalar field coupled to gravity with dynamics described by the action

$$S = \int d^4x \sqrt{-g} \left\{ \frac{M_{\text{Pl}}^2}{2} R - \frac{1}{2} (\partial h)^2 - V_{\text{eff}}(h) \right\}. \quad (\text{A.1})$$

$V_{\text{eff}}(h)$ is the effective potential which we assume to have the form of Eq. (6). We are interested in the era when the negative quartic term in $V_{\text{eff}}(h)$ dominates the vacuum energy V_0 , or in other words, when $V_{\text{eff}} < 0$. During this period, the bubble interior can be approximated by an FRW open universe. Then, the background metric has the form of Eq. (3) and using the equations of motion Eqs. (4) and (5), we find that

$$a'' = -\frac{a}{3M_{\text{Pl}}^2} [(h')^2 - V_{\text{eff}}] < 0, \quad (\text{A.2})$$

which implies that the scale factor is concave. Hence, the scale factor increases at the beginning, it reaches a maximum and then it decreases. Similarly, multiplying Eq. (4) by h' we get Eq. (9) and, therefore, the energy $\rho = (h')^2/2 + V_{\text{eff}}$ is increasing in the contracting ($a' < 0$) or decreasing in the expanding ($a' > 0$) phase. At this point one may ask if a singularity forms during the evolution of the universe. This happens if the conditions of Penrose's theorem are satisfied. The latter ensures that a spacetime cannot be null geodesically complete if the following conditions are fulfilled:

- 1) the spacetime has a closed trapped surface,
- 2) the spacetime has a non-compact Cauchy hypersurface,
- 3) the spacetime Ricci tensor satisfies $R_{\mu\nu} k^\mu k^\nu \geq 0$ for all null vectors k^μ .

Let us start with condition 1) by considering null vectors ℓ^μ and n^μ such that

$$\ell^\mu \ell_\mu = 0, \quad \ell^\mu \nabla_\mu \ell^\nu = 0, \quad n^\mu n_\mu = 0, \quad \ell^\mu n_\mu = -1. \quad (\text{A.3})$$

We define then the expansions θ_ℓ and θ_n as

$$\theta_\ell = \left(g^{\mu\nu} + \ell^\mu n^\nu + \ell^\nu n^\mu \right) \nabla_\mu \ell_\nu, \quad \theta_n = \left(g^{\mu\nu} + \ell^\mu n^\nu + \ell^\nu n^\mu \right) \nabla_\mu n_\nu. \quad (\text{A.4})$$

A trapped surface [35, 36] exists if the expansions θ_ℓ and θ_n for (future-directed) out-going ℓ^μ and in-going n^μ null geodesic congruences, respectively, satisfy [37]

$$\theta_\ell < 0 \text{ and } \theta_n < 0. \quad (\text{A.5})$$

For a spacetime described by a metric

$$ds^2 = -d\eta^2 + A^2(\eta, \chi)d\chi^2 + B^2(\eta, \chi)d\Omega_2^2, \quad (\text{A.6})$$

the conditions (A.5) turn out to be

$$\pm \frac{1}{A} \frac{\partial B}{\partial \chi} + B' < 0. \quad (\text{A.7})$$

For the metric in Eq. (3), this condition translates into

$$a' \pm \coth \chi < 0. \quad (\text{A.8})$$

Then, since $\coth \chi \geq 1$, we find that trapped surface is always formed when [34]

$$a' < -1. \quad (\text{A.9})$$

In our case, the evolution of the universe driven by the scalar field h is the following: at the initial time $\eta = 0$, a bubble is created, which then starts expanding. During its expansion, the scalar field energy density decreases. At a certain point the scale factor reaches a maximum at the moment when $a' = 0$, after which the universe starts contracting. During the contraction phase, the energy density increases unboundedly as we approach $a = 0$. This implies that a' is always decreasing, and at a certain point it will turn less than -1 , satisfying the apparent horizon condition of Eq. (A.9) for sufficiently large χ . Therefore, an apparent horizon will be formed and a trapped surface will always exist.

Condition 2) is also satisfied as it is known that a spacetime with metric of the form of Eq. (3) is globally hyperbolic [38] and therefore it has a (non-compact) Cauchy hypersurface.

Finally, from the Einstein equations one can easily show that, for any null vector k^μ , the Ricci tensor satisfies the inequality

$$R_{\mu\nu}k^\mu k^\nu = \frac{1}{M_{\text{Pl}}^2} \left(k^\mu \partial_\mu h \right)^2 \geq 0, \quad (\text{A.10})$$

satisfying the last condition 3). Therefore, all conditions of the Penrose's theorem are fulfilled and the considered spacetime is geodesically incomplete. This implies that the spacetime described by the metric (3) will sooner or later end up in a big crunch singularity during the Higgs dynamics.

B Initial radius outside the de Sitter Hubble radius

The analysis of Section 3 applies rigorously only to the case in which the initial radius of the bubble is smaller than $1/H_0$. In the case in which the bubbles form with an initial size larger than the Hubble radius, the external metric can be taken to be

$$ds_+^2 = -dt^2 + e^{2H_0 t} (d\rho^2 + \rho^2 d\Omega_2^2), \quad r > 1/H_0. \quad (\text{B.1})$$

This time the bubble is located at

$$\chi = X(\tau), \quad (\text{B.2})$$

as seen from the inside geometry and at

$$\rho = r(\tau) \quad (\text{B.3})$$

from the outside geometry. The induced metrics on the bubble from the two sides are

$$d\sigma_-^2 = -\left(\dot{T}_-^2 - a^2 \dot{X}^2\right) d\tau^2 + a^2 S^2(X) d\Omega_2^2, \quad (\text{B.4})$$

and

$$d\sigma_+^2 = -\left(\dot{T}_+^2 - e^{2H_0 T_+} \dot{r}^2\right) d\tau^2 + e^{2H_0 T_+} r^2 d\Omega_2^2. \quad (\text{B.5})$$

The two metrics (B.4) and (B.5) should coincide with the intrinsic bubble metric of Eq. (25). This leads to the conditions

$$\dot{T}_-^2 - a^2 \dot{X}^2 = 1, \quad (\text{B.6})$$

$$\dot{T}_+^2 - e^{2H_0 T_+} \dot{r}^2 = 1, \quad (\text{B.7})$$

$$R = aS = e^{H_0 T_+} r. \quad (\text{B.8})$$

We obtain

$$n_-^\mu = \left(a\dot{X}, \frac{T_-}{a}, 0, 0\right), \quad n_+^\mu = \left(e^{H_0 T_+} \dot{r}, \frac{\dot{T}_+}{e^{H_0 T_+}}, 0, 0\right), \quad (\text{B.9})$$

and

$$K_{\theta\theta}^+ = e^{H_0 T_+} r \dot{T}_+ + H_0 r^2 e^{3H_0 T_+} \dot{r}, \quad K_{\phi\phi}^+ = \sin^2 \theta K_{\theta\theta}^+. \quad (\text{B.10})$$

Correspondingly, the Israel matching turns out to be

$$e^{H_0 T_+} r \dot{T}_+ + H_0 r^2 e^{3H_0 T_+} \dot{r} - \dot{T}_- a S \frac{\partial S}{\partial \chi} - \dot{X} a' a^2 S^2 = -\frac{\sigma R^2}{2M_{\text{Pl}}^2}, \quad (\text{B.11})$$

which can be written as

$$\dot{T}_+ + H_0 r e^{2H_0 T_+} \dot{r} - \dot{T}_- \frac{\partial S}{\partial \chi} - \dot{X} a' a S = -\frac{\sigma R}{2M_{\text{Pl}}^2}. \quad (\text{B.12})$$

From Eq. (B.8) we find that

$$\begin{aligned}\dot{X} &= \frac{1}{a^2 \left(\frac{\partial S}{\partial \chi}\right)} \left(-a' \dot{T}_- R + a \dot{R}\right), \\ \dot{r} &= e^{-H_0 T_+} \left(\dot{R} - H_0 R \dot{T}_+\right),\end{aligned}\tag{B.13}$$

so that Eqs. (B.6) and (B.7) are written now as

$$\dot{T}_-^2 - \frac{1}{\left(\frac{\partial S}{\partial \chi}\right)^2} \left(-\frac{a'}{a} \dot{T}_- R + \dot{R}\right)^2 = 1,\tag{B.14}$$

$$\dot{T}_+^2 - \left(\dot{R} - H_0 R \dot{T}_+\right)^2 = 1.\tag{B.15}$$

Solving Eqs. (B.14) and (B.15) for \dot{T}_- and \dot{T}_+ , and using Eq. (B.13) in the Israel matching condition (B.12), we finally get

$$\left(\dot{R}^2 + 1 + \frac{R^2}{a^2} - \frac{a'^2}{a^2} R^2\right)^{1/2} = \epsilon \left(1 - H_0^2 R^2 + \dot{R}^2\right)^{1/2} + \frac{\sigma R}{2M_{\text{Pl}}^2}.\tag{B.16}$$

We notice that for $R > 1/H_0$ the system of Eqs. (B.14-B.16) reproduces Eqs. (50-52) as for large radii the term proportional to M/R can be neglected. Clearly, if the bubble collapses for a de Sitter space, it will also collapse for a Schwarzschild-de Sitter space. The reason is that, if the bubble collapses against the repulsive de Sitter force $\sim H^2 R$, will do the same when the collapse is assisted by an attractive GM/R^2 force when the bubble mass is positive.

C Comparison with the past literature

In this Appendix we wish to compare our results with those found in Ref. [11]. There it was assumed that in the interior of the bubble the geometry was exactly anti-de Sitter with a cosmological constant given by $-V_{\text{in}}$, corresponding to the length scale $1/\ell_{\text{in}}^2 = (V_{\text{in}}/3M_{\text{Pl}}^2)$, and in the exterior with a cosmological constant given by V_{out} , corresponding to the length scale $1/\ell_{\text{out}}^2 = (V_{\text{out}}/3M_{\text{Pl}}^2)$. It was found there that bubbles of anti-de Sitter expand in a Minkowski spacetime if $1/\ell_{\text{in}}^2 > (\sigma^2/4M_{\text{Pl}}^4)$ for two cases: either the initial radius is large, or it is small but the initial velocity is large enough. In the first case, independently from the bubble mass M , one has at large radii

$$\dot{R}^2 + V = -1 \quad \text{and} \quad V \simeq -k_3 R^2,\tag{C.1}$$

which can be integrated immediately to give

$$R(\tau) \sim \frac{1}{\sqrt{k_3}} \cosh\left(\sqrt{k_3} \tau\right).\tag{C.2}$$

In the second case we have

$$\dot{R}^2 + V = -1 \quad \text{and} \quad V \simeq -\frac{k_1}{R^4}, \quad (\text{C.3})$$

whose solution is

$$R(\tau) \sim k_1^{1/6} \tau^{1/3}. \quad (\text{C.4})$$

Let us show how to reproduce these results starting from the basic Eq. (56). Let us first consider the case of large radii, for which one can neglect the bubble mass, and reproduce Eq. (C.2). One obtains⁵

$$a(\eta) = \ell_{\text{in}} \sin \frac{\eta}{\ell_{\text{in}}}, \quad \rho = -\frac{3M_{\text{Pl}}^2}{\ell_{\text{in}}^2}, \quad \rho_c = \frac{3}{4} \frac{\sigma^2}{M_{\text{Pl}}^2} + \frac{M_{\text{Pl}}^2}{\ell_{\text{out}}^2}, \quad k_1 = k_2 \simeq 0, \quad (\text{C.5})$$

$$\begin{aligned} k_3 &= -\frac{1}{\ell_{\text{in}}^2} + \frac{1}{9\sigma^2} \left(3M_{\text{Pl}}^2 \left(\frac{1}{\ell_{\text{out}}^2} + \frac{1}{\ell_{\text{in}}^2} \right) + \frac{3}{4} \frac{\sigma^2}{M_{\text{Pl}}^2} \right)^2 \\ &= +\frac{1}{\ell_{\text{out}}^2} + \frac{1}{9\sigma^2} \left(3M_{\text{Pl}}^2 \left(\frac{1}{\ell_{\text{out}}^2} + \frac{1}{\ell_{\text{in}}^2} \right) - \frac{3}{4} \frac{\sigma^2}{M_{\text{Pl}}^2} \right)^2 \\ &\simeq \frac{M_{\text{Pl}}^6}{V_{\text{in}}} > 0. \end{aligned} \quad (\text{C.6})$$

Close to the coordinate singularity (which we set at $\eta = 0$) one can approximate $a(\eta) \sim \eta$, and assuming $R \gtrsim 1/\sqrt{k_3}$, Eq. (56) is written

$$R' \approx \left(k_3 R - \frac{1}{R} \pm \sqrt{k_3(k_3 R^2 - 1)} \right) \eta, \quad (\text{C.7})$$

which goes to zero close to the turning point at $R = 1/\sqrt{k_3}$. Expanding around the turning point, we find that the solution is approximately

$$R(\eta) \approx \frac{1}{\sqrt{k_3}} \left(1 + \frac{k_3^2}{8} \eta^4 \right), \quad (\text{C.8})$$

showing that the bubble radius expands. We can now solve directly the equations of motion for the bubble, which for the present case are written as

$$\dot{T}_-^2 - \frac{1}{1 + \frac{R^2}{T_-^2}} \left(-\frac{1}{T_-} \dot{T}_- R + \dot{R} \right)^2 = 1. \quad (\text{C.9})$$

Using the above expression for $R(\tau)$ in Eq. (C.9) we find that

$$\dot{T}_- = \pm \frac{\cosh(\sqrt{k_3} \tau) [\sqrt{2k_3} T_-^2 + \sqrt{2} \cosh^2(\sqrt{k_3} \tau)]}{\sqrt{k_3} T_- \sqrt{1 + 2k_3 T_-^2 + \cosh(2\sqrt{k_3} \tau)}} - \frac{\sinh(2\sqrt{k_3} \tau)}{2\sqrt{k_3} T_-}. \quad (\text{C.10})$$

⁵Notice that AdS is not singular. Comparing to Eq. (A.9), one has $a' = \cos(\eta/\ell_{\text{in}}) \geq -1$ and therefore it does not have a closed trapped surface. The singularity is only a coordinate one.

We cannot integrate the above equation, but we can find the solution $\eta = T_-(\tau)$ close to $\eta = 0$, which turns out to be

$$\tau = \pm \frac{\sqrt{k_3}}{2} T_-^2. \quad (\text{C.11})$$

Therefore, the solution for the wall radius close to $\eta = 0$ is written as

$$R \approx \frac{1}{\sqrt{k_3}} \left(1 + \frac{k_3}{2} \tau^2 \right) = \frac{1}{\sqrt{k_3}} \left(1 + \frac{k_3^2}{8} \eta^4 \right), \quad (\text{C.12})$$

which coincides with Eq. (C.8).

For small radii, Eq. (56) reduces to (selecting the + sign)

$$R' \simeq 2 \frac{k_1}{R^5} \eta, \quad (\text{C.13})$$

which is solved by

$$R(\eta) \sim k_1^{1/6} \eta^{1/3} \sim \ell_{\text{in}}^{2/3} \eta^{1/3}. \quad (\text{C.14})$$

The corresponding equation for T_- reads

$$\dot{T}_- = \frac{-(k_1/\tau)^{1/3} + \sqrt{[9 + (k_1/\tau^4)^{1/3}][T_-^2 + (k_1\tau^2)^{1/3}]}}{3T_-}, \quad (\text{C.15})$$

which can be solved close to $\eta = 0$ to find

$$T_- = \sqrt{\frac{3}{2}} \tau, \quad (\text{C.16})$$

reproducing therefore the behaviour found in Eq. (C.4). The maximum of the barrier is at $R_{\text{max}} \sim \ell_{\text{in}}/(\ell_{\text{in}} M_{\text{Pl}})^{2/3}$, which is reached within a time $\tau \sim \ell_{\text{in}}/(\ell_{\text{in}} M_{\text{Pl}})^2 \ll \ell_{\text{in}}$, signalling that the bubble wall passes the maximum of the potential and expands.

The basic difference among the results of Ref. [11] and the present paper is due to the time dependence of the potential V : when the dynamics of the Higgs is included, it changes the dynamics of the bubble wall, creating a sort of attractor solution which obliges the bubble wall to evolve as the internal scale factor, thus leading to its collapse before the end of inflation.

References

- [1] D. Buttazzo, G. Degrassi, P.P. Giardino, G.F. Giudice, F. Sala, A. Salvio et al., *Investigating the near-criticality of the Higgs boson*, *JHEP* **12** (2013) 089 [[1307.3536](#)].
- [2] G. Degrassi, S. Di Vita, J. Elias-Miro, J.R. Espinosa, G.F. Giudice, G. Isidori et al., *Higgs mass and vacuum stability in the Standard Model at NNLO*, *JHEP* **08** (2012) 098 [[1205.6497](#)].

- [3] J. Elias-Miro, J.R. Espinosa, G.F. Giudice, G. Isidori, A. Riotto and A. Strumia, *Higgs mass implications on the stability of the electroweak vacuum*, *Phys. Lett. B* **709** (2012) 222 [[1112.3022](#)].
- [4] PARTICLE DATA GROUP collaboration, *Review of Particle Physics*, *PTEP* **2020** (2020) 083C01.
- [5] CMS collaboration, *A profile likelihood approach to measure the top quark mass in the lepton+jets channel at $\sqrt{s} = 13$ TeV*, .
- [6] J.R. Espinosa, M. Garny, T. Konstandin and A. Riotto, *Gauge-Independent Scales Related to the Standard Model Vacuum Instability*, *Phys. Rev. D* **95** (2017) 056004 [[1608.06765](#)].
- [7] D.H. Lyth and A. Riotto, *Particle physics models of inflation and the cosmological density perturbation*, *Phys. Rept.* **314** (1999) 1 [[hep-ph/9807278](#)].
- [8] J.R. Espinosa, G.F. Giudice and A. Riotto, *Cosmological implications of the Higgs mass measurement*, *JCAP* **05** (2008) 002 [[0710.2484](#)].
- [9] M. Herranen, T. Markkanen, S. Nurmi and A. Rajantie, *Spacetime curvature and the Higgs stability during inflation*, *Phys. Rev. Lett.* **113** (2014) 211102 [[1407.3141](#)].
- [10] A. Hook, J. Kearney, B. Shakya and K.M. Zurek, *Probable or Improbable Universe? Correlating Electroweak Vacuum Instability with the Scale of Inflation*, *JHEP* **01** (2015) 061 [[1404.5953](#)].
- [11] J.R. Espinosa, G.F. Giudice, E. Morgante, A. Riotto, L. Senatore, A. Strumia et al., *The cosmological Higgstory of the vacuum instability*, *JHEP* **09** (2015) 174 [[1505.04825](#)].
- [12] T. Markkanen, A. Rajantie and S. Stopyra, *Cosmological Aspects of Higgs Vacuum Metastability*, *Front. Astron. Space Sci.* **5** (2018) 40 [[1809.06923](#)].
- [13] P. Burda, R. Gregory and I. Moss, *Gravity and the stability of the Higgs vacuum*, *Phys. Rev. Lett.* **115** (2015) 071303 [[1501.04937](#)].
- [14] P. Burda, R. Gregory and I. Moss, *Vacuum metastability with black holes*, *JHEP* **08** (2015) 114 [[1503.07331](#)].
- [15] N. Tetradis, *Black holes and Higgs stability*, *JCAP* **09** (2016) 036 [[1606.04018](#)].
- [16] D. Canko, I. Gialamas, G. Jelic-Cizmek, A. Riotto and N. Tetradis, *On the Catalysis of the Electroweak Vacuum Decay by Black Holes at High Temperature*, *Eur. Phys. J. C* **78** (2018) 328 [[1706.01364](#)].
- [17] A. Joti, A. Katsis, D. Loupas, A. Salvio, A. Strumia, N. Tetradis et al., *(Higgs) vacuum decay during inflation*, *JHEP* **07** (2017) 058 [[1706.00792](#)].

- [18] G. Franciolini, G.F. Giudice, D. Racco and A. Riotto, *Implications of the detection of primordial gravitational waves for the Standard Model*, *JCAP* **05** (2019) 022 [[1811.08118](#)].
- [19] G.N. Felder and I. Tkachev, *LATTICEEASY: A Program for lattice simulations of scalar fields in an expanding universe*, *Comput. Phys. Commun.* **178** (2008) 929 [[hep-ph/0011159](#)].
- [20] G.N. Felder, L. Kofman and A.D. Linde, *Tachyonic instability and dynamics of spontaneous symmetry breaking*, *Phys. Rev. D* **64** (2001) 123517 [[hep-th/0106179](#)].
- [21] J.R. Espinosa, D. Racco and A. Riotto, *Cosmological Signature of the Standard Model Higgs Vacuum Instability: Primordial Black Holes as Dark Matter*, *Phys. Rev. Lett.* **120** (2018) 121301 [[1710.11196](#)].
- [22] G.N. Felder, A.V. Frolov, L. Kofman and A.D. Linde, *Cosmology with negative potentials*, *Phys. Rev. D* **66** (2002) 023507 [[hep-th/0202017](#)].
- [23] W. Israel, *Singular hypersurfaces and thin shells in general relativity*, *Nuovo Cim. B* **44S10** (1966) 1.
- [24] S.K. Blau, E.I. Guendelman and A.H. Guth, *The Dynamics of False Vacuum Bubbles*, *Phys. Rev. D* **35** (1987) 1747.
- [25] R. Penrose, *Gravitational collapse: The role of general relativity*, *Riv. Nuovo Cim.* **1** (1969) 252.
- [26] C.D. Carone and A.H. Guth, *The Dynamics of Thick Domain Walls in an Inhomogeneous Inflationary Model*, *Phys. Rev. D* **42** (1990) 2446.
- [27] D. Garfinkle and R. Gregory, *Corrections to the Thin Wall Approximation in General Relativity*, *Phys. Rev. D* **41** (1990) 1889.
- [28] C. Barrabes, B. Boisseau and M. Sakellariadou, *Gravitational effects on domain walls with curvature corrections*, *Phys. Rev. D* **49** (1994) 2734 [[gr-qc/9307008](#)].
- [29] S. Khosravi, S. Khakshournia and R. Mansouri, *Evolution of thick walls in curved spacetimes*, *Class. Quant. Grav.* **23** (2006) 5927 [[gr-qc/0602063](#)].
- [30] B. Freivogel, G.T. Horowitz and S. Shenker, *Colliding with a crunching bubble*, *JHEP* **05** (2007) 090 [[hep-th/0703146](#)].
- [31] A.D. Linde, *Fast roll inflation*, *JHEP* **11** (2001) 052 [[hep-th/0110195](#)].
- [32] J. Kearney, H. Yoo and K.M. Zurek, *Is a Higgs Vacuum Instability Fatal for High-Scale Inflation?*, *Phys. Rev. D* **91** (2015) 123537 [[1503.05193](#)].

- [33] R. Alves Batista et al., *EuCAPT White Paper: Opportunities and Challenges for Theoretical Astroparticle Physics in the Next Decade*, [2110.10074](#).
- [34] L.F. Abbott and S.R. Coleman, *The Collapse of an Anti-de Sitter Bubble*, *Nucl. Phys. B* **259** (1985) 170.
- [35] R. Penrose, *Gravitational collapse and space-time singularities*, *Phys. Rev. Lett.* **14** (1965) 57.
- [36] S.W. Hawking and G.F.R. Ellis, *The Large Scale Structure of Space-Time*, Cambridge Monographs on Mathematical Physics, Cambridge University Press (2, 2011), [10.1017/CBO9780511524646](#).
- [37] I. Booth, *Black hole boundaries*, *Can. J. Phys.* **83** (2005) 1073 [[gr-qc/0508107](#)].
- [38] J.K. Beem, P. Ehrlich and K. Easley, *Global Lorentzian Geometry*, CRC Press (3, 1996).